The Influence of Alpha-Element Abundance on Planet Populations and Composition

Research Thesis

Presented in partial fulfillment of the requirements for graduation
with Research Distinction in Astronomy and Astrophysics in the undergraduate colleges of The Ohio State University

by

Brendan Kirsh

The Ohio State University
April 2024

Project Advisor: Professor Ji Wang, Department of Astronomy

Draft version April 29, 2024
Typeset using LaTeX **twocolumn** style in AASTeX63

The Influence of Alpha-Element Abundance on Planet Populations and Composition

Brendan R. Kirsh[1]

[1] *Department of Astronomy, The Ohio State University, Columbus, OH 43210, USA*

ABSTRACT

The exact mechanisms of planetary formation remains one of the dominant areas of research in planetary astronomy. Though there are extant prevailing theories (e.g., pebble accretion, core accretion, etc.) for different planets, degeneracies between these theories can make it difficult to resolve how exactly a particular planet formed, or to make predictions on what conditions might be favorable for planet formation. Though the effect of host star metallicity on planet occurrence rates and the correlation between metallicity and planet mass have been well-established, the effect of stellar elemental abundances, particularly that of α-elements, remains comparatively less studied. The goal of this study is to examine planetary compositions, particularly those of rocky planets, through the lens of elemental abundances of their host stars. We determine a functional form $[\alpha/\mathrm{Fe}] = Ae^{B\cdot[\mathrm{Fe/H}]+C} + D$ with fitting parameters A = 0.083, B = -2.025, C = -0.140, and D = -0.046 that describes the value of α-element abundance as a function of metallicity and determine an overall negative correlation between α-element abundance and metallicity for all planet populations except Sub-Saturns due to lack of available metallicity data. Using the planetary interior modeling software `ExoPlex`, we determine a strong positive correlation between core mass fraction (CMF) and surface gravity, with planetary mass correlating to a combination of these variables.

Keywords: planets and satellites: composition, planets and satellites: interiors, planets and satellites: rocky planets, density, Super-Earth

1. INTRODUCTION

The methods by which planetary systems come into formation and align themselves into their orbits after the protoplanetary disk stage are confounded by an assortment of variables; the different theories of planet formation currently have degeneracies between them. While this study does not venture to resolve these issues, we do aim to provide insight into the influence that elemental and mineral composition have on the planet that is formed.

It is well-established that there is a wide variety of planet classifications that eclipses even what we see in our own solar system; planets of varying mass and radius have been discovered throughout the galaxy (NASA Exoplanet Archive 2024; Bashi & Zucker 2021). Given the number of exoplanets detected, several studies have investigated the diversity of planet populations and their formation mechanisms. There is a noted diversity in the composition of planets, both interior and atmospheric, with particular focus on that of rocky planets (Bond et al. 2010; Schulze et al. 2021; Rodríguez-Martínez 2023). Resolving the internal composition of exoplanets involves understanding the availability of major rock-building elements present at the time of planet formation, as the delivery of these materials is thought to affect the variety of planet composition that we see (Venturini et al. 2020). Initial theory predicts that there should be a relationship between the compositions of exoplanets and their host stars, as they both form via accretion of the same materials from a surrounding protoplanetary disk. Studies in recent years have examined the efficacy of analyzing the chemical abundances of a planet's host star to determine the composition of the planet itself; there is a correlation between the host star and rocky planet composition, and past studies show that the host star's composition reflects the planet's to a strong degree (Adibekyan et al. 2021a; Schulze et al. 2021). Because the compositions of host stars can be resolved with stellar abundances inferred through spectroscopic observations, these chemical abundances are often used as proxies for the analysis of exoplanet abundances (Adibekyan et al. 2021b).

kirsh.17@osu.edu

The effect of host star metallicity on planet formation is well-established (Fischer & Valenti 2005; Udry & Santos 2007; Petigura et al. 2018; Zink et al. 2023). Past studies have established mass-metallicity trends, particularly for giant planets (Teske et al. 2019; Sun et al. 2024). Studies have shown that the presence of increased metallicity increases the likelihood that planets will form around a host star, indicating a direct correlation between metallicity and planet occurrence (Fischer & Valenti 2005; Wang & Fischer 2014). The planet-metallicity correlation is well-established in giant planets, which show a strong correlation with metal-rich material (Fischer & Valenti 2005; Petigura et al. 2018; Zink et al. 2023); this correlation appears significantly weaker for smaller planets (Petigura et al. 2018; Zink et al. 2023), except at metallicities below -0.5 dex (Boley et al. (2024) submitted). Stars hosting sub-Neptunes and super-Earths display metallicities that are typical of stars without planets (Udry et al. 2006; Sousa et al. 2008; Ghezzi et al. 2010; Mayor et al. 2011; Sousa et al. 2011). Though the effect host star metallicity has on the formation of their resultant planetary system is well-understood, the effect of other elemental abundances, such as α-elements, remains unclear. α-elements are both the products and reactants of the α-process, a class of nuclear fusion reaction by which helium is converted into heavier elements. Past studies have identified a systematic overabundance of α-elements in exoplanet-hosting stars as compared to similar stars that do not host planets, with α-enrichment most evident at metallicities below -0.3 dex (Adibekyan et al. 2012), so there is motivation for determining a relationship between α-element abundance and exoplanet occurrence.

The goal of this study is to quantitatively constrain the dependence of planet populations on α-elements. We do this by determining a sample of confirmed exoplanets that we can cross-match with host stars that have available elemental abundance data for iron and a selection of α-elements, which we can utilize to determine a functional form between metallicity and α-element abundance. Given the already-established link between exoplanet occurrence and host star metallicity, this will constrain the ratio of abundances necessary for planet formation around a star. Additionally, we define a sub-sample of likely rocky planets, with which we use `ExoPlex`[1] (Unterborn et al. 2018; Unterborn & Panero 2019; Unterborn et al. 2022) to model the interiors of the planets in this sub-sample by inputting the known abundances of their host stars. Given that rocky planet compositions are correlated with host star elemental abundances, we aim to quantitatively address the impact of stellar abundances on the composition of such planets. This will provide insight into the relationship between host star abundance and rocky planet composition.

The outline of our paper is as follows. Section 2 describes the determination of the stars we use to resolve the abundances of our sample of planets. Section 3 describes the determination of the planet sample itself and later our utilization of `ExoPlex` to determine the parameters of a sub-sample of Super-Earths. In Section 4, we provide the results of the determined functional form describing the relationship between metallicity and α-element abundance, and the planetary interiors as modeled by `ExoPlex`. We discuss our results as compared to other studies and the limitations of the interior modeling software in Section 5, along with possible future avenues of study. Finally, we provide a summary and conclude in Section 6.

2. ACQUIRING STELLAR ABUNDANCES

We begin by establishing a collection of stars with well-determined chemical abundances to allow us to analyze the abundances and internal compositions of exoplanets. We use the results from three spectroscopic surveys: GALAH DR3 (Buder et al. 2021), APOGEE DR17 (Abdurro'uf et al. 2022), and LAMOST DD-Payne, a subsample of LAMOST DR5 (Xiang et al. 2019). We apply the following series of cuts to the stellar data:

1. **General quality cuts:** We begin by making initial cuts to the stellar catalogs based on signal-to-noise ratios, goodness-of-fit (based on χ^2 test results), and other stellar parameter quality flags included in the catalogs. A breakdown of the flags used in each survey is as follows:
   (a) GALAH: We begin by setting the `flap_sp` flag to zero to eliminate entries with identified problems in the determination of their stellar parameters. We ensure the original data had decent signal-to-noise in each channel by setting the flags `snr_c1_iraf`, `snr_c2_iraf`, `snr_c3_iraf`, and `snr_c4_iraf` all to be greater than 20.
   (b) APOGEE: Similar to the stellar parameter flag for GALAH, we require `ASPCAPFLAG` to be equal to zero, and the `SNR` flag to be greater than 20 to ensure decent signal-to-noise.
   (c) LAMOST: We require the quality flag `QFLAG_CHI2` to equal 'g' for 'good', and again

[1] https://github.com/CaymanUnterborn/ExoPlex/

require the signal-to-noise `SNR_G` to be greater than 20.

2. **Surface gravity:** We avoid complications introduced by low surface gravity red giants by excluding stars with $\log g > 4.1$.

3. **Abundance quality flags:** Each catalog contains quality flags pertaining to the reported abundances. We exclude stars that have a flag indicating issues with the determination of the [Fe/H], [Mg/Fe], [Si/Fe], [Al/Fe] and [Ca/Fe] abundances. These are given as the following flags in each of the surveys:

   (a) GALAH: We require the `flag_Mg_fe`, `flag_Si_fe`, `flag_Al_fe`, `flag_Ca_fe`, `flag_fe_h` and `flag_alpha_fe` flags to all be equal to zero.

   (b) APOGEE: We require the `MG_FE_FLAG`, `SI_FE_FLAG`, `AL_FE_FLAG`, `CA_FE_FLAG`, and `FE_H_FLAG` flags to all be equal to zero.

   (c) LAMOST: We require the `MG_FE_FLAG`, `SI_FE_FLAG`, `AL_FE_FLAG`, `CA_FE_FLAG`, and `FEH_FLAG` flags to all be equal to one, in accordance to the convention established in Xiang et al. (2019).

Performing these cuts leaves us with 1,984,273 stars, which we can cross-match with the NASA Exoplanet Archive (NEA) to define our planet sample (more details in the following section). The primary focus of our analysis involves examining the composition of the planets in our sample through the lens of elemental abundances, specifically looking at the relationship between α-element abundance, [α/Fe], and metallicity, [Fe/H]. APOGEE does not have an [α/Fe] column, instead reporting [α/M] and [M/H] abundances, with M representing heaving elements that are considered metals. We are able to use the properties of logarithms to define an [α/Fe] column within APOGEE by taking

$$[\alpha/\mathrm{Fe}] = [\alpha/\mathrm{M}] + [\mathrm{M/H}] - [\mathrm{Fe/H}]. \quad (1)$$

We will later use the [Fe/Mg], [Si/Mg], [Al/Mg], and [Ca/Mg] abundances, which we can find by taking

$$[\mathrm{Fe/Mg}] = -[\mathrm{Mg/Fe}] \quad (2)$$

and

$$[\mathrm{X/Mg}] = [\mathrm{X/Fe}] - [\mathrm{Mg/Fe}], \quad (3)$$

where X is the element whose abundance we are interested in finding relative to Mg.

We perform a cross-calibration of the surveys, inspired by the procedure in Soubiran et al. (2022), to account for systematic offset in the abundance measurements across the different surveys. As the largest of the three stellar abundance catalogs, we consider LAMOST to be our "base" catalog to which we scale the abundances of the other catalogs to. To compare how metallicity and α-element abundance are resolved between surveys with shared stellar data, we select stars in GALAH and APOGEE that are common in LAMOST based off of Gaia DR3 IDs. We then use the `optimize.curve_fit` routine within SciPy to perform a non-linear least squares fit of the non-LAMOST [Fe/H] data on the x-axis (e.g. $[\mathrm{Fe/H}]_{\mathrm{GALAH}}$) and the difference between the LAMOST [Fe/H] data and the non-LAMOST [Fe/H] data on the y-axis (e.g. $[\mathrm{Fe/H}]_{\mathrm{GALAH}} - [\mathrm{Fe/H}]_{\mathrm{LAMOST}}$) to a linear function. This returns a function that gives the offset between the different surveys' [Fe/H] abundance as a function of [Fe/H] for common stars, which we can generalize and apply to the entire survey. This allows us to more reliably treat all of the stellar data as if it is from the same survey before we cross-match it with the exoplanetary data.

3. PLANET SAMPLE

To construct our sample of planets, we use the exoplanet data available from the NEA catalog, first removing any planets that are flagged as controversial. We then drop planets that do not have radius values or measured orbital periods associated with them, as we use these values to determine the class of planet we are considering. The NEA catalog of roughly 5,600 planets contains multiple entries from different sources for many of the planets, so we remove duplicate entries for each planet by defining a relative uncertainty in the radius values. We do this by taking the average of the magnitudes of the upper and lower uncertainties and dividing by the corresponding radius value. The entry with the lowest relative radius uncertainty for each set of entries for a planet is thus chosen as our ideal candidate, leaving us with a portion of the NASA Exoplanet Archive's confirmed planets. We cross-match our planet sample with the LAMOST, GALAH, and APOGEE surveys to identify host star-planet pairs, resulting in 781 planets with abundance values that also have determined radii and orbital periods. After cross-matching to determine our planet sample, we define the following four planet populations within our sample:

1. Super-Earths: defined in accordance to the cut described by Ho & Van Eylen (2023); to characterize the small planet radius valley, i.e., the apparent scarcity of planets with radii measured between

1.5 and 2 R⊕, as publicized in Fulton et al. (2017), Ho and Van Eylen determined a functional form that describes the boundary between the bimodality in the size of small exoplanets. The Ho and Van Eylen cut describes a maximum radius for which a planet can be classified as a Super-Earth as a function of its orbital period. The cut defines a maximum radius in Earth radii

$$R_{max} = 10^{m \cdot \log(P/\text{days}) + c} \tag{4}$$

with $m = -0.11$ and $c = 0.37$; P is the orbital period of the planet in days. If the planet's calculated radius is less than R_{max}, we consider it a Super-Earth; we resolve 282 Super-Earths in our sample.

2. Sub-Neptunes: defined as a planet whose radius exceeds that specified by the Ho & Van Eylen cut but is no greater than 4 $R_\oplus$; we resolve 320 Sub-Neptunes in our sample.

3. Sub-Saturns: defined to have a radius between 4-8 $R_\oplus$; we resolve 71 Sub-Saturns in our sample.

4. Jupiters: defined to have radii greater than or equal to 8 $R_\oplus$; we resolve 108 Jupiters in our sample.

We define our sub-samples of planet classes based on the previously mentioned radius cuts so we can later analyze how planetary parameters change based on these classes.

3.1. *Interior Compositions*

We utilize `ExoPlex` as the base of our planet interior model, a thermodynamically self-consistent planet interior software (Unterborn et al. 2018; Unterborn & Panero 2019; Unterborn et al. 2022). `ExoPlex` solves five coupled differential equations: the mass within a sphere, hydrostatic equilibrium, adiabatic temperature profile, Gauss' law of gravity in one dimension, and the thermally-dependent equation of state for solid planets. We use a version of `ExoPlex` with modified code that uses the following inputs: planet mass, planet radius (so as to constrain the calculated radius value), equilibrium temperature, and the Fe, Si, Al, and Ca molar abundances relative to Mg. These limited parameters can be used by `ExoPlex` to return information on planetary parameters like density, core mass fraction (i.e., the fraction of the planet's mass that is composed of its core), the pressure/temperature in the planets core, and the pressure/temperature at the boundary between the planet's core and mantle, all of which fit the composition modelled by the software.

`ExoPlex` makes use of the Fe, Si, Al, and Ca abundances relative to Mg of the planet whose interior we wish to model; however, these abundances (quoted in brackets) are given as the star's logarithmic abundances relative to the Sun, while `ExoPlex` uses the molar abundance ratios of the stars themselves. We thus must decompose the given relative abundance values of each star into their respective molar abundance ratios using established literature values for the Sun's molar abundances; we follow the treatment as described by Hinkel et al. (2022), using the present-day solar photosphere abundances provided in Asplund, M. et al. (2021). We recover the molar abundance ratios via the relation

$$\frac{\mathrm{N_X}}{\mathrm{N_{Mg}}} = 10^{[\mathrm{X/Mg}] + \log\left(\frac{\mathrm{N_X}}{\mathrm{N_{Mg}}}\right)_\odot}, \tag{5}$$

where $\mathrm{N_X}$ represents the molar abundance for the element X. We define this value for each planet in our sample using the logarithmic abundance ratios as reported by each of the stellar surveys.

The applications of `ExoPlex` are limited to rocky planets; we thus want to define a sub-sample of our sample of Super-Earths that we can feed into `ExoPlex` to model their interior compositions. We want to augment the accuracy of the composition calculations made by `ExoPlex` by making cuts to our Super-Earth sample based on uncertainty in the mass and radius determinations. In the previous section, we determined the relative uncertainty in the mass and radius of each planet entry and kept the entry with the best radius measurement for each planet; for the purposes of `ExoPlex`, Super-Earths whose best radius uncertainty is greater than 10 are excluded outright. With our main planet sample, we were not concerned with the uncertainty in mass; `ExoPlex` however relies on an accurate mass measurement in order to model the planetary interiors. We require a relative mass uncertainty of less than 30% for our sub-sample; we also require the `pl_bmassprov` parameter within the NEA to take the value "Mass" to ensure that the reported mass is from an actual mass measurement, and not calculated based on inclination (e.g., $M \sin i$). Exoplanets with mass measurements (especially of the provenance we require) are exceedingly rare, so this cut removes a vast majority of the Super-Earths from our sub-sample; we also drop Super-Earths with masses greater than 10 $M_\oplus$ due to limitations of `ExoPlex`. This leaves us with a sub-sample of 19 Super-Earths to be evaluated by `ExoPlex`.

4. RESULTS

4.1. *[α/Fe] vs. [Fe/H] Functional Form*

With our sample of planets, we use the `optimize.curve_fit` routine within SciPy to perform

a non-linear least squares fit to an exponential function of the form

$$f(x) = Ae^{Bx+C} + D \tag{6}$$

where the variables A, B, C, and D are left as fitting parameters. In this case, x represents the [Fe/H] abundances and $f(x)$ represents the [α/Fe] abundances of the planets. Fitting our planetary sample to this function returns the values A = 0.083, B = -2.025, C = -0.140, and D = -0.046, with the fitting parameters rounded to three decimal places for conciseness. Figure 1 presents our planet sample on an [α/Fe] vs. [Fe/H] plot, with the functional form described by Equation 6 represented by a dashed red line. We perform a fit to the same function in Equation 6 using only our sub-sample of Super-Earths to determine if there is a significant difference in the relationship between α-element abundance and metallicity for Super-Earths as compared to exoplanets as a whole. We determine the following values for Super-Earths: A = 0.130, B = -1.313, C = -0.065 and D = -0.092, again with the fitting parameters rounded to three decimal places for conciseness. This function is also represented on Figure 1 via a dashed green line. The α-element abundance for the planet sample as a whole appears to have a slightly steeper dependence on metallicity than the Super-Earths alone.

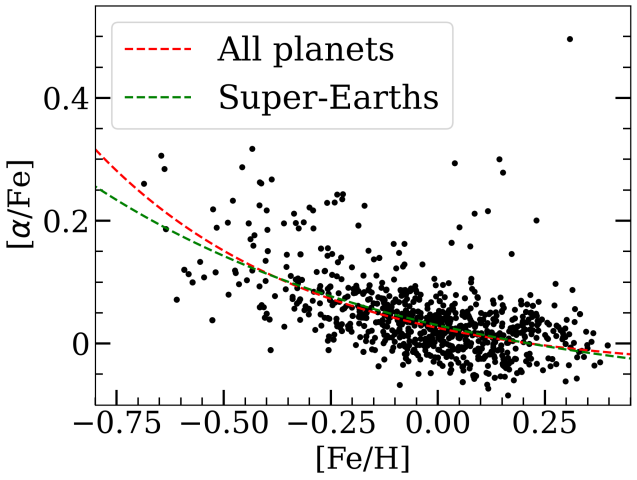

Figure 1: Curves given by the inputting the fitting parameters into Equation 6, recovered by fitting [α/Fe] vs. [Fe/H] data for the planet sample and the Super-Earths sub-sample to Equation 6. The red dashed line represents the fit performed on the planet sample as a whole. The green line represents this fit when performed on only Super-Earths. The black dots represent the individual planets in our sample.

4.2. *Planetary Properties*

We present in this section the plots comparing α-element abundance as a function of metallicity for each of the sub-samples of planet type, as seen in Figure 2. For each planet class except Super-Earths (Sub-Neptunes, Sub-Saturns, and Jupiters) we color the data points based on their mean density in g/cm^3, calculated via the masses and radii reported by the NEA. For Sub-Neptunes and Jupiters, we notice an overall negative correlation between α-element abundance and metallicity, which is consistent with our results from curve fitting in the previous section. This correlation is not evident in our population of Sub-Saturns, however the elemental abundance data is more limited for this population. The correlation between α-element abundance and metallicity typically becomes apparent at metallicities below -0.3 dex, while the minimum [Fe/H] value for our Sub-Neptunes only reaches -0.155 dex. Though we colored the data points by the mean density of these planets, there doesn't appear to be any noticeable correlation between a planet's mean density and α-element abundance or metallicity.

For Super-Earths, we plot only the sub-sample of entries that had their interiors modelled by `ExoPlex`, as seen in Figure 2a; we color the data points based on their core mass fractions as calculated by `ExoPlex`. Similar to the other classes of planets, we notice an overall negative correlation between α-element abundance and metallicity that is consistent with our findings from the previous section. Like the coloring by density for the other planet populations, we do not see an apparent correlation between CMF and the metallicity of α-element abundance.

We present for Super-Earths another plot that shows surface gravity g as a function of CMF, with the data points colored by the planet's mass as reported by the NEA. Surface gravity has been calculated using the formula

$$g = \frac{GM}{R^2} \tag{7}$$

where G is the gravitational constant and M and R are the masses and radii as reported by the NEA, respectively. We notice a strong positive correlation between surface gravity and core mass fraction, with g appearing to increase linearly with an increase in CMF. We also note the apparent correlation of planetary mass to the planet's location on the surface gravity vs. CMF plot; that is, there appear to be regimes of planet masses that follow diagonal lines across the plot.

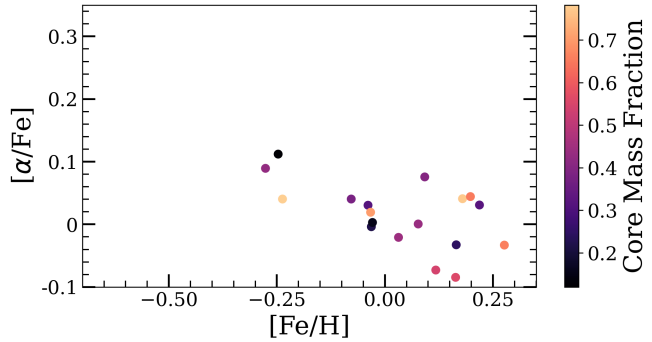

(a) α-element abundance vs. metallicity for Super-Earths, with coloring by core mass fraction as returned by `ExoPlex`.

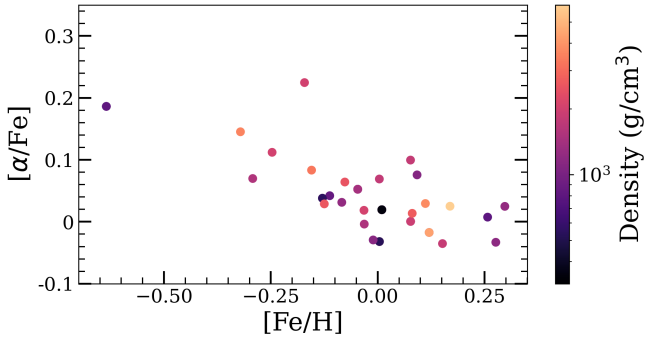

(b) α-element abundance vs. metallicity for Sub-Neptunes, with coloring by density.

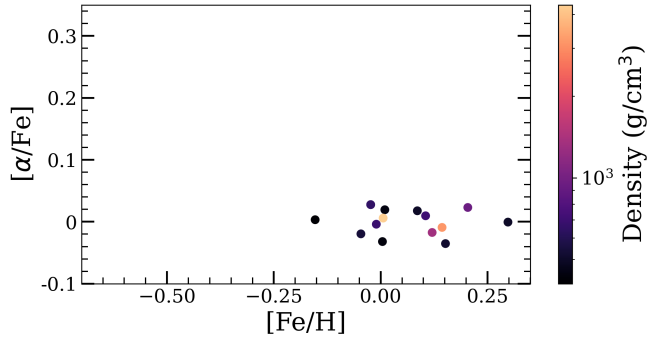

(c) α-element abundance vs. metallicity for Sub-Saturns, with coloring by density.

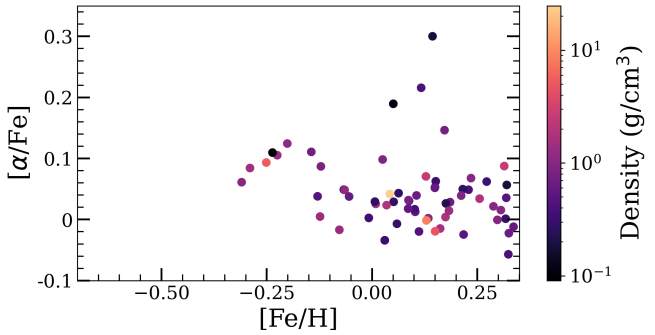

(d) α-element abundance vs. metallicity for Jupiters, with coloring by density.

Figure 2: α-element abundance vs. metallicity plots for each of the planet types we've classified.

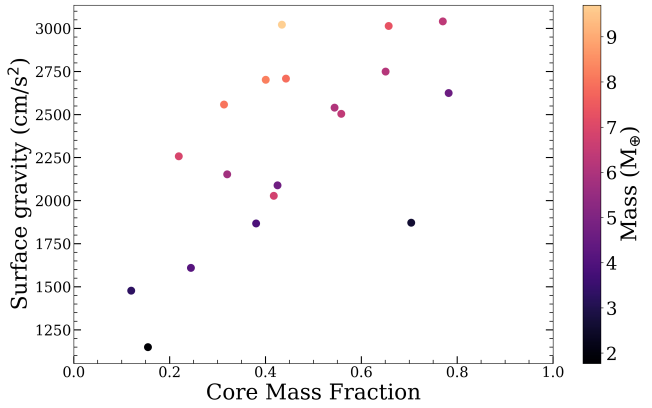

Figure 3: Surface gravity g plotted as a function of CMF as modelled by `ExoPlex`. Data points are colored by planet mass in Earth masses as reported by the NEA.

5. DISCUSSION

We determined the functional forms of [α/Fe] as a function of [Fe/H] for our entire planet sample and for only Super-Earths and found that the α-element abundance of the planet sample as a whole had a slightly steeper dependence on metallicity than Super-Earths alone. This suggests that Super-Earths tend to have less α-element enrichment than their larger exoplanet counterparts; this may lead to the conclusion that α-elements have a role in planet formation and may be a strong component in planet-building materials. This is supported by previous studies that note an overabundance of α-elements in planet-hosting stars when compared to similar stars without planets (Adibekyan et al. 2012).

As noted in the previous section, we did not determine there to be a strong correlation between density and α-element abundance or metallicity. This is interesting because it suggests that while elemental abundance might affect the size of planet that is initially formed, these abundances might not have a large affect on the actual composition of the planets once they have formed. Likewise for the Super-Earths, there was no discernible correlation between core mass fraction and the α-element abundance or metallicity. Based on the fact that the planet-metallicity correlation is much weaker for non-giant planets, this lack of correlation in Super-Earths is not particularly surprising. We instead note the strong

positive correlation between core mass fraction and surface gravity, as seen in Figure 3. There is also an evident linear relationship between a planet's placement on the g vs. CMF plot and its mass, as we see a moderately smooth gradient in the planet mass moving down and rightwards across the plot, with apparent iso-mass profiles present. This behavior is explainable through the interplay of mass, radius, and composition; while maintaining a constant mass, decreased radius leads to increased surface gravity and increased density, thereby increasing the CMF as well. Thus, a point with constant mass will move up on both axes in a linear fashion. Further study of this revelation will be necessary to understand how the discretization of the masses along linear profiles relates to surface gravity and core mass fraction as more planetary data with masses and abundances to input into `ExoPlex` become available.

The limitations of the `ExoPlex` software imposed a number of restrictions on the planets whose interiors we could model and required us to make a number of assumptions to allow our sub-sample to be used. `ExoPlex` is currently limited in its ability to model the interiors of particularly massive rocky planets, so we had to disregard Super-Earths whose masses exceeded 10 $M_\oplus$. We also chose not take into account the potential atmospheres of the planets we modelled with the software. A rocky planet's radius is considered to consist of both its solid surface and its atmosphere, so planets with considerably large atmospheres could have a large affect on its density and could potentially confound the calculation of its core mass fraction. A study that is less focused on the internal composition of rocky planets and instead focuses on atmospheric composition would be more well-suited to take this factor into account.

This study also does not consider the affect of irradiation from host stars on the composition of rocky planets. Planets that are particularly close-in to their host stars may be sufficiently irradiated to cause melting in their surfaces and mantles, resulting in magma oceans that could affect planet structure and evolution (Boley et al. 2023; Falco et al. 2024). The study of these lava world has recently emerged and is yet to be well-understood, but provides yet another potential avenue of understanding for Super-Earths.

Continued work on this topic would likely benefit from considering elemental abundances through the lens of other variables, such as galactic location. It has been well-established through studies over the past few decades that stellar elemental abundance has a dependence on galactic location (Bensby et al. 2003). Extending the logic from this study and the research that inspired it, one could expect planet occurrence to depend on location in the galaxy and its influence on the elemental abundance of potential host stars. As such, there are studies on the direct correlation between galactic location and planet occurrence rates (Bashi & Zucker 2021; Zink et al. 2023). Previous studies have also considered the effects of the presence of multiple planets in a system on planetary composition (Rodríguez Martínez et al. 2023), which may be another variable of interest when looking at how planet composition might be affected by having to share available planet-building materials with other planets in a system.

6. SUMMARY & CONCLUSIONS

The exact mechanisms of planet formation are still grappled with by researchers today. Though prevailing theories have been determined by researchers, these theories often have degeneracies between them that further confound the issue. Given the limited sample size of our own solar system, the study of exoplanets provides a unique insight into the result of these planet formation processes in various locations throughout the galaxy. Looking into the interior compositions of planets through the lens of host star elemental abundances is a promising avenue that could reveal fundamental information on how the presence of potential planet-building materials affect the means by which planets come to be.

From this study, we present our primary conclusions:

1. We determine a functional form that describes the relationship between α-element abundance and metallicity for a sample of 781 planets with radii values that have been cross-matched with stellar surveys (Equation 6).

2. We determine a similar functional form describing the relationship between α-element abundance and metallicity for a sub-sample of Super-Earths. We note the steeper dependence on metallicity for the planet sample as a whole when compared to that of the Super-Earth sub-sample, suggesting a relationship between planet size and α-element abundance. These functions allow us to create predictions on the α-element enrichment of a planet based on its metallicity (i.e., that of its host star), which could help to constrain predictions in the sizes of planets that might form around stars depending on their metallicities.

3. In plotting individual planet classes, we determine an overall negative correlation between α-element abundance and metallicity, except for Sub-Saturns, which had insufficient metallicity data to determine any correlation. We do not resolve any significant correlation between planet

density and α-element abundance or metallicity. Similarly, for Super-Earths in particular we do not resolve any significant correlation between core mass fraction and α-element abundance or metallicity.

4. We determine a strong positive correlation between surface gravity and core mass fraction, with an apparent linear relationship in g as a function of CMF. We also note the correlation that is apparent between planetary mass and its location on this surface gravity vs. core mass fraction plot.

7. ACKNOWLEDGMENTS

This research has made use of the NASA Exoplanet Archive, which is operated by the California Institute of Technology, under contract with the National Aeronautics and Space Administration under the Exoplanet Exploration Program.

This work made use of the Third Data Release of the GALAH Survey (Buder et al. 2021).

Guoshoujing Telescope (the Large Sky Area Multi-Object Fiber Spectroscopic Telescope LAMOST) is a National Major Scientific Project built by the Chinese Academy of Sciences. Funding for the project has been provided by the National Development and Reform Commission. LAMOST is operated and managed by the National Astronomical Observatories, Chinese Academy of Sciences.

Funding for the Sloan Digital Sky Survey IV has been provided by the Alfred P. Sloan Foundation, the U.S. Department of Energy Office of Science, and the Participating Institutions. SDSS-IV acknowledges support and resources from the Center for High Performance Computing at the University of Utah. The SDSS website is www.sdss4.org.

Software: `ExoPlex` (Unterborn et al. 2018; Unterborn & Panero 2019; Unterborn et al. 2022), `TOPCAT` (Taylor 2005, 2006)

REFERENCES

Abdurro'uf, Accetta, K., Aerts, C., et al. 2022, ApJS, 259, 35, doi: 10.3847/1538-4365/ac4414

Adibekyan, V., Dorn, C., Sousa, S. G., et al. 2021a, Science, 374, 330332, doi: 10.1126/science.abg8794

Adibekyan, V., Santos, N. C., Dorn, C., et al. 2021b, Communications of the Byurakan Astrophysical Observatory, 447453, doi: 10.52526/25792776-2021.68.2-447

Adibekyan, V. Z., Santos, N. C., Sousa, S. G., et al. 2012, Astronomy amp; Astrophysics, 543, A89, doi: 10.1051/0004-6361/201219564

Asplund, M., Amarsi, A. M., & Grevesse, N. 2021, AA, 653, A141, doi: 10.1051/0004-6361/202140445

Bashi, D., & Zucker, S. 2021, Monthly Notices of the Royal Astronomical Society, 510, 3449, doi: 10.1093/mnras/stab3596

Bensby, T., Feltzing, S., & Lundström, I. 2003, A&A, 410, 527, doi: 10.1051/0004-6361:20031213

Boley, K., Christiansen, J., Zink, J., et al. 2024, in AAS/Division for Extreme Solar Systems Abstracts, Vol. 56, AAS/Division for Extreme Solar Systems Abstracts, 301.02

Boley, K. M., Panero, W. R., Unterborn, C. T., et al. 2023, Fizzy Super-Earths: Impacts of Magma Composition on the Bulk Density and Structure of Lava Worlds. https://arxiv.org/abs/2307.13726

Bond, J. C., O' Brien, D. P., & Lauretta, D. S. 2010, The Astrophysical Journal, 715, 10501070, doi: 10.1088/0004-637x/715/2/1050

Buder, S., Sharma, S., Kos, J., et al. 2021, MNRAS, 506, 150, doi: 10.1093/mnras/stab1242

Falco, A., Tremblin, P., Charnoz, S., Ridgway, R. J., & Lagage, P.-O. 2024, Hydrogenated atmospheres of lava planets: atmospheric structure and emission spectra. https://arxiv.org/abs/2401.14744

Fischer, D. A., & Valenti, J. 2005, The Astrophysical Journal, 622, 1102, doi: 10.1086/428383

Fulton, B. J., Petigura, E. A., Howard, A. W., et al. 2017, The Astronomical Journal, 154, 109, doi: 10.3847/1538-3881/aa80eb

Ghezzi, L., Cunha, K., Smith, V. V., et al. 2010, ApJ, 720, 1290, doi: 10.1088/0004-637X/720/2/1290

Hinkel, N. R., Young, P. A., & Wheeler III, C. H. 2022, The Astronomical Journal, 164, 256, doi: 10.3847/1538-3881/ac9bfa

Ho, C. S. K., & Van Eylen, V. 2023, Monthly Notices of the Royal Astronomical Society, 519, 4056, doi: 10.1093/mnras/stac3802

Mayor, M., Marmier, M., Lovis, C., et al. 2011, The HARPS search for southern extra-solar planets XXXIV. Occurrence, mass distribution and orbital properties of super-Earths and Neptune-mass planets. https://arxiv.org/abs/1109.2497

NASA Exoplanet Archive. 2024, Planetary Systems, Version: 2024-01-26 07:32, NExScI-Caltech/IPAC, doi: 10.26133/NEA12

Petigura, E. A., Marcy, G. W., Winn, J. N., et al. 2018, AJ, 155, 89, doi: 10.3847/1538-3881/aaa54c

Rodríguez-Martínez, R. 2023, in American Astronomical Society Meeting Abstracts, Vol. 55, American Astronomical Society Meeting Abstracts, 145.02D

Rodríguez Martínez, R., Martin, D. V., Gaudi, B. S., et al. 2023, AJ, 166, 137, doi: 10.3847/1538-3881/aced9a

Schulze, J. G., Wang, J., Johnson, J. A., et al. 2021, , 2, 113, doi: 10.3847/PSJ/abcaa8

Soubiran, C., Brouillet, N., & Casamiquela, L. 2022, A&A, 663, A4, doi: 10.1051/0004-6361/202142409

Sousa, S. G., Santos, N. C., Israelian, G., Mayor, M., & Udry, S. 2011, A&A, 533, A141, doi: 10.1051/0004-6361/201117699

Sousa, S. G., Santos, N. C., Mayor, M., et al. 2008, A&A, 487, 373, doi: 10.1051/0004-6361:200809698

Sun, Q., Wang, S. X., Welbanks, L., Teske, J., & Buchner, J. 2024, A revisit of the Mass-Metallicity Trends in Transiting Exoplanets. https://arxiv.org/abs/2402.08292

Taylor, M. B. 2005, in Astronomical Society of the Pacific Conference Series, Vol. 347, Astronomical Data Analysis Software and Systems XIV, ed. P. Shopbell, M. Britton, & R. Ebert, 29

Taylor, M. B. 2006, in Astronomical Society of the Pacific Conference Series, Vol. 351, Astronomical Data Analysis Software and Systems XV, ed. C. Gabriel, C. Arviset, D. Ponz, & S. Enrique, 666

Teske, J. K., Thorngren, D., Fortney, J. J., Hinkel, N., & Brewer, J. M. 2019, The Astronomical Journal, 158, 239, doi: 10.3847/1538-3881/ab4f79

Udry, S., & Santos, N. C. 2007, ARA&A, 45, 397, doi: 10.1146/annurev.astro.45.051806.110529

Udry, S., Mayor, M., Benz, W., et al. 2006, A&A, 447, 361, doi: 10.1051/0004-6361:20054084

Unterborn, C. T., Desch, S. J., Haldemann, J., et al. 2022, arXiv e-prints, arXiv:2212.03934, doi: 10.48550/ARXIV.2212.03934

Unterborn, C. T., Desch, S. J., Hinkel, N. R., & Lorenzo, A. 2018, Nature Astronomy, 2, 297, doi: 10.1038/s41550-018-0411-6

Unterborn, C. T., & Panero, W. R. 2019, Journal of Geophysical Research (Planets), 124, 1704, doi: 10.1029/2018JE005844

Venturini, J., Ronco, M. P., & Guilera, O. M. 2020, Space Science Reviews, 216, doi: 10.1007/s11214-020-00700-y

Wang, J., & Fischer, D. A. 2014, The Astronomical Journal, 149, 14, doi: 10.1088/0004-6256/149/1/14

Xiang, M., Ting, Y.-S., Rix, H.-W., et al. 2019, ApJS, 245, 34, doi: 10.3847/1538-4365/ab5364

Zink, J. K., Hardegree-Ullman, K. K., Christiansen, J. L., et al. 2023, AJ, 165, 262, doi: 10.3847/1538-3881/acd24c